Analytical model for PEM fuel cell concentration impedance

Andrei Kulikovsky[a)]
Theory and Computation of Energy Materials (IEK–13)
Institute of Energy and Climate Research
Forschungszentrum Jülich GmbH
D–52425 Jülich, Germany [b)]

(Dated: 30 August 2021)

Analytical model for concentration/pressure (zeta) impedance of the cathode side of a PEM fuel cell is developed. The model is based on transient oxygen mass transport equations through the gas–diffusion and cathode catalyst layers. Analytical solution for zeta–impedance is derived and the relation of zeta–impedance and regular cell impedance is obtained. In the limit of high oxygen consumption in the catalyst layer, simple equations for the static point of zeta impedance are derived. These equations allow one to estimate oxygen transport coefficients of the catalyst and gas diffusion layers from the static point of zeta–spectrum. Qualitative resemblance of the model and experimental zeta–spectrum is demonstrated.

Keywords: PEM fuel cell, concentration impedance, modeling

I. INTRODUCTION

In PEM fuel cells, potential, current and oxygen concentration are strongly coupled due to the oxygen reduction reaction (ORR) on the cathode; hence perturbation of any of the three parameters perturbs the other two. The idea to perturb fuel cell potential/current by applying harmonic perturbation of the oxygen concentration δc or pressure δp has been suggested in[1] and elaborated further in[2–5].

Dividing amplitude of the cell voltage response by δc one gets the concentration impedance, or simply zeta–impedance. The great advantage of this technique is that under certain conditions, zeta–spectrum is insensitive to faradaic processes in a cell (see below). This feature makes pressure/concentration impedance spectroscopy a powerful tool for studying oxygen transport in PEMFCs, especially in the regimes when the characteristic frequency of oxygen transport is close to the ORR frequency.

The concentration/pressure impedance spectroscopy of fuel cells is an emerging field and only a few publications are devoted to this topic. Niroumand et al.[1] applied pressure perturbation to the cell outlet and measured cell voltage response. They suggested to use this technique for understanding liquid water transport in the cell. Engebretsen et al.[2] applied pressure perturbations to the whole cathode flow field using loudspeaker and measured the response of cell voltage in a wide range of perturbation frequencies and cell current densities. A qualitative diagnostics of water management in the cell using this method has been demonstrated. Sorrentino et al.[3] developed a general model for concentration–alternating frequency response analysis (cFRA) and illustrated this model by numerical calculations of concentration–potential and concentration–current spectra of a PEM fuel cell. Later, Sorrentino et al.[6] measured cFRA and EIS spectra of a PEM fuel cell and reported qualitative comparison of the two spectra types. Shirsath et al.[4] measured standard EIS and pressure–impedance spectra and reported higher sensitivity of pressure impedance to water transport in the cell. Kubannek and Krewer[5] measured perturbation of CO_2 flux from the methanol oxidation reaction (MOR) induced by the perturbation of electrode potential. They developed numerical model to analyze MOR kinetics from experimental frequency response data. Kulikovsky[7], has made attempt to construct analytical model for PEM fuel cell concentration impedance. However, the Nyquist spectra derived in[7] do not agree with the recent experiments. Recently, a correction to Ref.[7] has been published[8], which explains the reason for faulty final equation for the zeta–impedance.

Calculation of concentration/pressure impedance is under–determined problem. The electric impedance of a PEM fuel cell is calculated from the solution of linearized equation for ORR overpotential perturbation. This problem is well–determined in a sense that the equation and boundary conditions do not contain undefined parameters. On the contrary, the concentration impedance ζ appears in the ODE as a boundary condition. To calculate ζ one, therefore, needs an additional closing relation, which introduces unknown model parameter to the problem. Below, we providing arguments that in a high–current regime of cell operation this model parameter can be set to zero, making the procedure of concentration impedance calculation fully determined. This idea leads to zeta–spectra, which closely resemble the shape of experimental spectra. A review of pressure impedance literature can be found in[4,9].

[a)] Electronic mail: A.Kulikovsky@fz-juelich.de
[b)] Also at: Lomonosov Moscow State University, Research Computing Center, 119991 Moscow, Russia

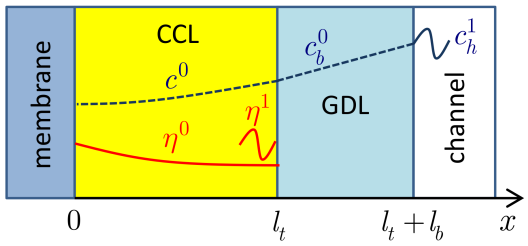

FIG. 1. Schematic of the cell transport layers and the through–plane static shapes of the oxygen concentration c and ORR overpotential η (Ref.[7]). Oscillations of η^1 occur in time, not in space.

A model for concentration impedance ζ of a PEM fuel cell cathode reported below takes into account oxygen transport in the cathode catalyst layer (CCL) and gas diffusion layer (GDL). A closed–form solutions for ζ–impedance are derived and relation of zeta–impedance and regular "electric" cell impedance is obtained. In the limit of large oxygen consumption in the cathode, analytical expressions for the static limit of zeta–impedance are derived. Finally, qualitative resemblance of the model and experimental zeta–spectrum[2] is demonstrated.

II. MODEL

The model is based on standard macro–homogeneous approximation for the cathode catalyst layer performance[10] and it employs the following assumptions.

- Air flow stoichiometry is large. This means that the characteristic frequency of oxygen transport in channel is large and it does not affect the zeta–spectra of GDL and CCL.
- Proton transport in the CCL is fast, meaning that the static η^0 and perturbed η^1 shapes of the ORR overpotential are nearly independent of $\tilde{x}$ (Figure 1).

The key assumption is the last one; it is fulfilled if the CCL proton conductivity is high so that the following relation holds: $j_0 \ll \sigma_p b/l_t$ (see discussion below). For notations please see Nomenclature section.

The model is based on the coupled oxygen mass transport equations in the CCL, Eq.(1), and in the GDL, Eq.(2):

$$\frac{\partial c}{\partial t} - D_{ox}\frac{\partial^2 c}{\partial x^2} = -\frac{i_*}{4F}\left(\frac{c}{c_h^{in}}\right)\exp\left(\frac{\eta}{b}\right) \tag{1}$$

$$\frac{\partial c_b}{\partial x} - D_b\frac{\partial^2 c_b}{\partial x^2} = 0 \tag{2}$$

Linearization and Fourier–transform of Eqs.(1), (2) lead to the system of linear equations for the small perturbation amplitudes $\tilde{c}^1$, $\tilde{c}_b^1$ and $\tilde{\eta}^1$ in the ω–space[11]:

$$\tilde{D}_{ox}\frac{\partial^2 \tilde{c}^1}{\partial \tilde{x}^2} = \mathrm{e}^{\tilde{\eta}^0}\left(\tilde{c}^1 + \tilde{c}^0\tilde{\eta}^1\right) + \mathrm{i}\tilde{\omega}\tilde{c}^1, \quad \left.\frac{\partial \tilde{c}^1}{\partial \tilde{x}}\right|_{\tilde{x}=0} = 0, \quad \tilde{c}^1(1) = \tilde{c}_b^1(1) \tag{3}$$

$$\tilde{D}_b\frac{\partial^2 \tilde{c}_b^1}{\partial \tilde{x}^2} = \mathrm{i}\tilde{\omega}\tilde{c}_b^1, \quad \tilde{D}_b\left.\frac{\partial \tilde{c}_b^1}{\partial \tilde{x}}\right|_{\tilde{x}=1+} = \tilde{D}_{ox}\left.\frac{\partial \tilde{c}^1}{\partial \tilde{x}}\right|_{\tilde{x}=1-}, \quad \tilde{c}_b^1(1+\tilde{l}_b) = \tilde{c}_h^1 \tag{4}$$

where the sign tilde marks the dimensionless variables defined according to

$$\tilde{x} = \frac{x}{l_t}, \quad \tilde{t} = \frac{t i_*}{4F c_h^{in}}, \quad \tilde{c} = \frac{c}{c_h^{in}}, \quad \tilde{\eta} = \frac{\eta}{b}, \quad \tilde{j} = \frac{j}{l_t i_*}, \quad \tilde{\omega} = \frac{\omega 4F c_h^{in}}{i_*}, \quad \tilde{D} = \frac{4FDc_h^{in}}{l_t^2 i_*}, \quad \tilde{\zeta} = \frac{\zeta c_h^{in}}{b}, \quad \tilde{Z} = \frac{Z l_t i_*}{b}. \tag{5}$$

Here D stands for D_{ox} and D_b, Z is the electric impedance, and the superscripts 0 and 1 mark the static shapes and the perturbation amplitudes, respectively.

The left boundary condition for Eq.(3) describes zero oxygen flux in membrane and the right boundary condition expresses continuity of the oxygen concentration at the CCL/GDL interface. The boundary conditions for Eq.(4) mean continuity of the oxygen flux at this interface and the fixed (applied) amplitude $\tilde{c}_h^1$ of the oxygen concentration perturbation in the air channel.

Eq.(4) can be directly solved leading to[12]

$$\tilde{c}_b^1(1) = -\alpha\tilde{D}_{ox}\frac{\partial\tilde{c}^1}{\partial\tilde{x}}\bigg|_{\tilde{x}=1-} + \beta\tilde{c}_h^1 \tag{6}$$

where

$$\alpha = \frac{\tanh\left(\tilde{l}_b\sqrt{\mathrm{i}\tilde{\omega}/\tilde{D}_b}\right)}{\sqrt{\mathrm{i}\tilde{\omega}\tilde{D}_b}}, \quad \beta = \frac{1}{\cosh\left(\tilde{l}_b\sqrt{\mathrm{i}\tilde{\omega}/\tilde{D}_b}\right)} \tag{7}$$

It is convenient to introduce zeta–admittance $\tilde{G}$:

$$\tilde{G}(\tilde{x}) = \frac{\tilde{c}^1(\tilde{x})}{\tilde{\eta}^1}, \tag{8}$$

Substituting Eq.(6) into the right boundary condition for Eq.(3) and dividing Eq.(3) by $\tilde{\eta}^1$, we get a problem for $\tilde{G}(\tilde{x})$:

$$\tilde{D}_{ox}\frac{\partial^2\tilde{G}}{\partial\tilde{x}^2} = \mathrm{e}^{\tilde{\eta}^0}\left(\tilde{G}+\tilde{c}^0\right) + \mathrm{i}\tilde{\omega}\tilde{G}, \quad \frac{\partial\tilde{G}}{\partial\tilde{x}}\bigg|_{\tilde{x}=0} = 0, \quad \tilde{G}(1) + \alpha\tilde{D}_{ox}\frac{\partial\tilde{G}}{\partial\tilde{x}}\bigg|_{\tilde{x}=1-} = \beta\tilde{G}_h \tag{9}$$

where $\tilde{G}_h = \tilde{c}_h^1/\tilde{\eta}^1 = 1/\tilde{\zeta}$ is the measurable value of $\tilde{G}$, which is of primary interest in this work.

The static shape of the oxygen concentration $\tilde{c}^0(\tilde{x})$ through the CCL depth obeys to equation

$$\tilde{D}_{ox}\frac{\partial^2\tilde{c}^0}{\partial\tilde{x}^2} = \tilde{c}^0\mathrm{e}^{\tilde{\eta}^0}, \quad \frac{\partial\tilde{c}^0}{\partial\tilde{x}}\bigg|_{\tilde{x}=0} = 0, \quad \tilde{c}^0(1) = \tilde{c}_1^0 \tag{10}$$

where $\tilde{c}_1^0$ is the static oxygen concentration at the CCL/GDL interface. Solution to Eq.(10) is

$$\tilde{c}^0 = \frac{\tilde{c}_1^0\cosh\left(\tilde{x}\sqrt{\mathrm{e}^{\tilde{\eta}^0}/\tilde{D}_{ox}}\right)}{\cosh\left(\sqrt{\mathrm{e}^{\tilde{\eta}^0}/\tilde{D}_{ox}}\right)}. \tag{11}$$

III. RESULTS AND DISCUSSION

A. General solution

Substituting Eq.(11) into Eq.(9) and solving the resulting equation, we get

$$\tilde{G}(\tilde{x}) = \frac{\left(\mathrm{e}^{\tilde{\eta}^0}\tilde{c}_1^0\left(\alpha\tilde{D}_{ox}\phi_0\tanh\phi_0+1\right)+\beta\tilde{G}_h\mathrm{i}\tilde{\omega}\right)\cosh(\phi_1\tilde{x})}{\mathrm{i}\tilde{\omega}\left(\alpha\tilde{D}_{ox}\phi_1\sinh\phi_1+\cosh\phi_1\right)} - \frac{\mathrm{e}^{\tilde{\eta}^0}\tilde{c}_1^0\cosh(\phi_0\tilde{x})}{\mathrm{i}\tilde{\omega}\cosh\phi_0} \tag{12}$$

where the auxiliary parameters ϕ_0 and ϕ_1 are given by

$$\phi_0 = \sqrt{\frac{\mathrm{e}^{\tilde{\eta}^0}}{\tilde{D}_{ox}}}, \quad \phi_1 = \sqrt{\frac{\mathrm{e}^{\tilde{\eta}^0}+\mathrm{i}\tilde{\omega}}{\tilde{D}_{ox}}}. \tag{13}$$

Measurable admittance $\tilde{G}_h$ appears on the right side of Eq.(12). Thus, to calculate $\tilde{G}_h$ we need a closing relation: $\tilde{c}^1(0) = \tilde{c}_0$, or $\tilde{G}(0) = \tilde{G}_0$. The value $\tilde{G}_0$ at the membrane surface can hardly be measured and hence the closing relation introduces a model parameter $\tilde{G}_0$ (see below). Setting in Eq.(12) $\tilde{x} = 0$, equating the resulting expression to $\tilde{G}_0$ and solving for $\tilde{G}_h$, we get the dimensionless zeta–impedance $\tilde{\zeta} = 1/\tilde{G}_h$:

$$\tilde{\zeta} = \frac{\mathrm{i}\tilde{\omega}\beta\cosh\phi_0}{\tilde{c}_1^0\mathrm{e}^{\tilde{\eta}^0}}\left(\left(\alpha\tilde{D}_{ox}\phi_1\sinh\phi_1+\cosh\phi_1\right)\left(1+\frac{\mathrm{i}\tilde{\omega}\tilde{G}_0\cosh\phi_0}{\tilde{c}_1^0\mathrm{e}^{\tilde{\eta}^0}}\right)-\alpha\tilde{D}_{ox}\phi_0\sinh\phi_0-\cosh\phi_0\right)^{-1} \tag{14}$$

Eq.(14) is the general solution for zeta–impedance of a PEM fuel cell cathode operating at high stoichiometry of the oxygen flow.

The contribution of oxygen transport in the GDL to $\tilde{\zeta}$ is taken into account by the coefficients α and β in the right boundary condition to Eq.(9). Infinite GDL oxygen diffusivity (zero GDL impedance) corresponds to $\alpha = 0$ and $\beta = 1$. Thus, setting $\alpha = 0$ and $\beta = 1$ in Eq.(14) we get zeta–impedance of the CCL only:

$$\tilde{\zeta}_{ccl} = \frac{\mathrm{i}\tilde{\omega}\cosh\phi_0}{\tilde{c}_1^0\mathrm{e}^{\tilde{\eta}^0}}\left(\left(1+\frac{\mathrm{i}\tilde{\omega}\tilde{G}_0\cosh\phi_0}{\tilde{c}_1^0\mathrm{e}^{\tilde{\eta}^0}}\right)\cosh\phi_1-\cosh\phi_0\right)^{-1} \tag{15}$$

B. Zeta–impedance and electric impedance

In the limit of fast proton transport in the CCL considered here, it is possible to establish relation between ζ–impedance and electric cell impedance Z. We begin with the proton current conservation equation in the CCL:

$$C_{dl}\frac{\partial\eta}{\partial t}+\frac{\partial j}{\partial x} = -i_*\left(\frac{c}{c_h^{in}}\right)\exp\left(\frac{\eta}{b}\right) \tag{16}$$

With the dimensionless variables, Eq.(5), Eq.(16) takes the form

$$\xi^2\frac{\partial\tilde{\eta}}{\partial\tilde{t}}+\frac{\partial\tilde{j}}{\partial\tilde{x}} = -\tilde{c}\exp\tilde{\eta}, \quad \text{where} \quad \xi = \sqrt{\frac{C_{dl}b}{4Fc_h^{in}}}. \tag{17}$$

Substituting $\tilde{\eta} = \tilde{\eta}^0 + \tilde{\eta}^1(\tilde{\omega})\exp(\mathrm{i}\tilde{\omega}\tilde{t})$, $\tilde{j} = \tilde{j}^0(\tilde{x}) + \tilde{j}^1(\tilde{x},\tilde{\omega})\exp(\mathrm{i}\tilde{\omega}\tilde{t})$, $\tilde{c} = \tilde{c}^0(\tilde{x}) + \tilde{c}^1(\tilde{x},\tilde{\omega})\exp(\mathrm{i}\tilde{\omega}\tilde{t})$ into Eq.(17), and taking into account smallness of perturbation amplitudes, at first order we get

$$\mathrm{i}\tilde{\omega}\xi^2\tilde{\eta}^1+\frac{\partial\tilde{j}^1}{\partial\tilde{x}} = -\mathrm{e}^{\tilde{\eta}^0}\left(\tilde{c}^1+\tilde{c}^0\tilde{\eta}^1\right) \tag{18}$$

where, by assumption $\tilde{\eta}^1$ is independent of $\tilde{x}$. Dividing this equation by $\tilde{\eta}^1$, and introducing electric admittance $\tilde{A} = \tilde{j}^1/\tilde{\eta}^1$, we get the linear problem for $\tilde{A}$:

$$\mathrm{i}\tilde{\omega}\xi^2+\frac{\partial\tilde{A}}{\partial\tilde{x}} = -\mathrm{e}^{\tilde{\eta}^0}\left(\tilde{G}+\tilde{c}^0\right), \quad \tilde{A}(1) = 0 \tag{19}$$

where $\tilde{G}$ and $\tilde{c}^0$ on the right side are given by Eqs.(12) and (11), respectively. Solving Eq.(19) and setting $\tilde{x} = 0$ in the solution, we find

$$\tilde{A}(0) = \mathrm{i}\tilde{\omega}\xi^2+\left(p\,\mathrm{e}^{\tilde{\eta}^0}\right)\frac{\sinh\phi_1}{\phi_1}+\tilde{c}_1^0\mathrm{e}^{\tilde{\eta}^0}\left(\frac{\mathrm{i}\mathrm{e}^{\tilde{\eta}^0}}{\tilde{\omega}}+1\right)\frac{\tanh\phi_0}{\phi_0} \tag{20}$$

where p is the coefficient at $\cosh(\phi_1\tilde{x})$ in Eq.(12):

$$p = \frac{\mathrm{e}^{\tilde{\eta}^0}\tilde{c}_1^0\left(\alpha\tilde{D}_{ox}\phi_0\tanh\phi_0+1\right)+\beta\tilde{G}_h\mathrm{i}\tilde{\omega}}{\mathrm{i}\tilde{\omega}\left(\alpha\tilde{D}_{ox}\phi_1\sinh\phi_1+\cosh\phi_1\right)} \tag{21}$$

The cathode electric impedance is

$$\tilde{Z} = \left.\frac{\tilde{\eta}^1}{\tilde{j}^1}\right|_{\tilde{x}=0} = \frac{1}{\tilde{A}(0)}. \tag{22}$$

Setting in Eq.(20) $\tilde{A}(0) = 1/\tilde{Z}$ and $\tilde{G}_h = 1/\tilde{\zeta}$, we get an algebraic equation relating $\tilde{Z}$ and $\tilde{\zeta}$. After simple algebra we finally find the relation of cathode zeta–impedance $\tilde{\zeta}$ and electric impedance $\tilde{Z}$:

$$\frac{1}{\tilde{\zeta}} - \frac{q\phi_1}{\beta \mathrm{e}^{\tilde{\eta}^0}\tilde{Z}} = -\frac{q\phi_1}{\beta}\left(\frac{\mathrm{i}\tilde{\omega}\xi^2}{\mathrm{e}^{\tilde{\eta}^0}} + \tilde{c}_1^0\left(\frac{\mathrm{i}\mathrm{e}^{\tilde{\eta}^0}}{\tilde{\omega}} + 1\right)\frac{\tanh\phi_0}{\phi_0}\right) + \frac{\mathrm{i}\mathrm{e}^{\tilde{\eta}^0}\tilde{c}_1^0}{\beta\tilde{\omega}}\left(\alpha\tilde{D}_{ox}\phi_0\tanh\phi_0 + 1\right) \tag{23}$$

where

$$q = \alpha\tilde{D}_{ox}\phi_1 + \coth\phi_1. \tag{24}$$

With $\alpha = 0$ and $\beta = 1$, Eq.(23) reduces to the relation of CCL zeta–impedance $\tilde{\zeta}_{ccl}$ and electric impedance $\tilde{Z}_{ccl}$:

$$\frac{1}{\tilde{\zeta}_{ccl}} - \frac{\phi_1}{\tanh(\phi_1)\mathrm{e}^{\tilde{\eta}^0}\tilde{Z}_{ccl}} = -\frac{\phi_1}{\tanh\phi_1}\left(\frac{\mathrm{i}\tilde{\omega}\xi^2}{\mathrm{e}^{\tilde{\eta}^0}} + \tilde{c}_1^0\left(\frac{\mathrm{i}\mathrm{e}^{\tilde{\eta}^0}}{\tilde{\omega}} + 1\right)\frac{\tanh\phi_0}{\phi_0}\right) + \frac{\mathrm{i}\tilde{c}_1^0\mathrm{e}^{\tilde{\eta}^0}}{\tilde{\omega}} \tag{25}$$

Eqs.(23) and (25) allow one to express $\tilde{\zeta}$ through $\tilde{Z}$ and vice versa.

C. Strong oxygen consumption in the CCL

Generally, when fitting experimental zeta–spectra, $\tilde{G}_0$ in Eq.(14) can be claimed as a fitting parameter. At present, the literature data on zeta–spectra are scarce and validity of this conjecture is difficult to verify. However, in the case of strong oxygen consumption in the CCL, $\tilde{G}_0$ could be set to zero, which greatly simplifies the analysis. With $\tilde{G}_0 = 0$, Eq.(14) simplifies to

$$\tilde{\zeta}^* = \frac{\mathrm{i}\tilde{\omega}\beta\cosh\phi_0}{\tilde{c}_1^0\mathrm{e}^{\tilde{\eta}^0}}\left(\alpha\tilde{D}_{ox}\left(\phi_1\sinh\phi_1 - \phi_0\sinh\phi_0\right) + \cosh\phi_1 - \cosh\phi_0\right)^{-1} \tag{26}$$

where the upper asterisk means that Eq.(26) is valid at a high rate of oxygen consumption in the CCL. This condition holds if the cell current density exceeds the characteristic current density j_{ox} for oxygen transport in the CCL:

$$j_0 \gtrsim j_{ox} = \frac{4FD_{ox}c_1^0}{l_t} \tag{27}$$

Importantly, Eq.(26) is obtained not using the charge conservation equation. Furthermore, from Eqs.(5) it follows that Eq.(26) does not contain double layer capacitance, meaning that the limiting zeta–impedance $\tilde{\zeta}^*$ is insensitive to the charge–transfer process. Thus, $\tilde{\zeta}^*$ is particularly useful when the charge–transfer and oxygen transport frequencies are close to each other and standard EIS cannot separate them.

In the limit of strong oxygen consumption, the CCL polarization curve is[13]

$$\tilde{j}_0 = \tilde{j}_{ox}\sqrt{\frac{\mathrm{e}^{\tilde{\eta}^0}}{\tilde{D}_{ox}}}, \quad \text{or} \quad \mathrm{e}^{\tilde{\eta}^0} = \tilde{D}_{ox}\left(\frac{\tilde{j}_0}{\tilde{j}_{ox}}\right)^2 \tag{28}$$

Eq.(28) allows us to express $\mathrm{e}^{\tilde{\eta}^0}$ through $\tilde{j}_0$ in Eq.(26).

Setting $\alpha = 0$ and $\beta = 1$ in Eq.(26) (a limit of zero GDL impedance), we get the CCL high–current concentration impedance:

$$\tilde{\zeta}_{ccl}^* = \frac{\mathrm{i}\tilde{\omega}\cosh\phi_0}{\tilde{c}_1^0\mathrm{e}^{\tilde{\eta}^0}\left(\cosh\phi_1 - \cosh\phi_0\right)} \tag{29}$$

The same result can be obtained by passing to the limit $\tilde{D}_b \to \infty$ in Eq.(26). The Nyquist plots of ζ^* and ζ_{ccl}^* are shown in Figure 2a; Figure 2b depicts the frequency dependencies of imaginary part of $\tilde{\zeta}$ and $\tilde{\zeta}_{ccl}$. Two distinct features are seen:

Tafel slope b, V	0.03
Exchange current density i_*, A cm^{-3}	10^{-3}
Oxygen diffusion coefficient in the CCL[14], D_{ox}, cm^2 s^{-1}	10^{-4}
Oxygen diffusion coefficient in the GDL[14], D_b, cm^2 s^{-1}	$2 \cdot 10^{-2}$
Catalyst layer thickness l_t, cm	$10 \cdot 10^{-4}$ (10 μm)
Gas diffusion layer thickness l_b, cm	$200 \cdot 10^{-4}$ (200 μm)
Cell current density j_0, A cm^{-2}	1.0
Pressure	Standard
Cell temperature T, K	273 + 80

TABLE I. The cell parameters used in calculations.

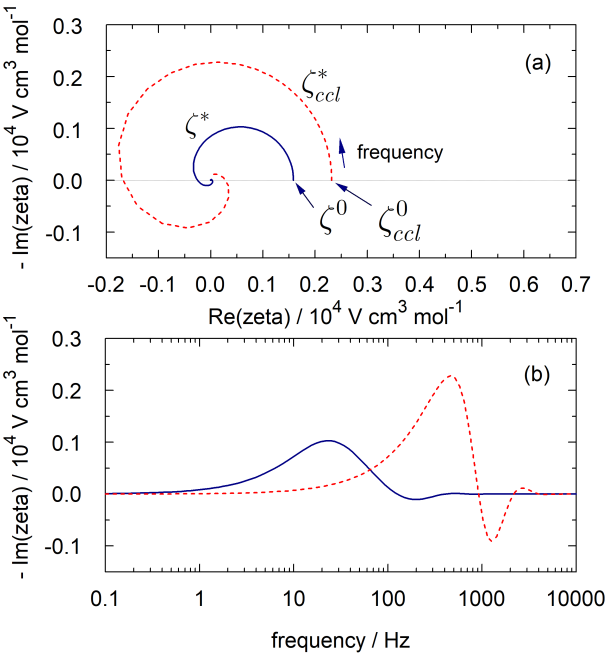

FIG. 2. (a) The Nyquist spectra of $\tilde{\zeta}$, Eq.(26) (solid line), and of $\tilde{\zeta}_{ccl}$, Eq.(29) (dashed line). $\tilde{\zeta}^0$ marks the static state of zeta–impedance. (b) The frequency dependence of imaginary part of impedances in (a). Parameters for the calculations are listed in Table I.

(i) the contribution of GDL oxygen transport reduces the diameter of the Nyquist curl (Figure 2a), and (ii) it lowers the characteristic frequency of the curl (the leftmost peak in Figure 2b). Note also that the systems reach the steady state at $f \simeq 0.1$ Hz (Figure 2b).

Position $f_{\max}$ of the leftmost peak of $-\operatorname{Im}(\zeta^*)$ on the frequency scale is proportional to the GDL oxygen diffusivity (Figure 3). However, the dependence of this peak frequency on the GDL thickness is *not* $f_{\max} \sim l_b^{-2}$, as one might expect by analogy with the Warburg finite–length formula. The linear dependence indicated in Figure 3 is valid for $l_b = 0.02$ cm; for other values of l_b the slope of the straight line is different. Quite analogous, position of the leftmost peak of $-\operatorname{Im}(\zeta^*_{ccl})$ on the frequency scale is proportional to the CCL oxygen diffusivity (Figure 4). Again, the parameters of fitting line in Figure 4 are valid for the CCL thickness of 10 μm; for other thicknesses the linear dependence would be different. Lowering of CCL oxygen diffusivity dramatically lowers the diameter of Nyquist arc and leads to formation of multiple high–frequency loops in the Nyquist spectrum (Figure 5). This feature is a qualitative signature of a low D_{ox} value.

The equations for static points $\tilde{\zeta}^0$ and $\tilde{\zeta}^0_{ccl}$ (Figure 2a) can be derived from Taylor series expansion of the functions $1/\tilde{\zeta}$

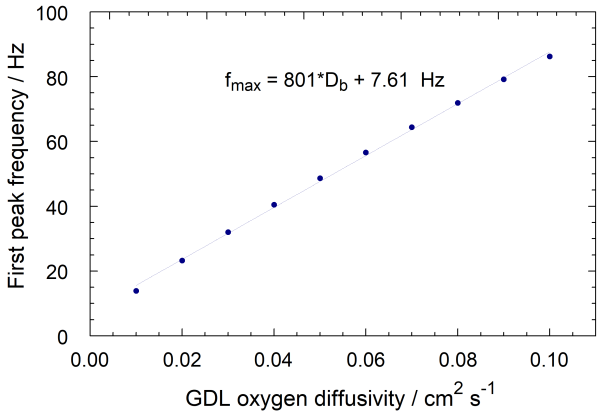

FIG. 3. Position of the first (leftmost) peak of $-\operatorname{Im}(\zeta^*)$ (Figure 2b) on the frequency scale vs. GDL oxygen diffusivity D_b.

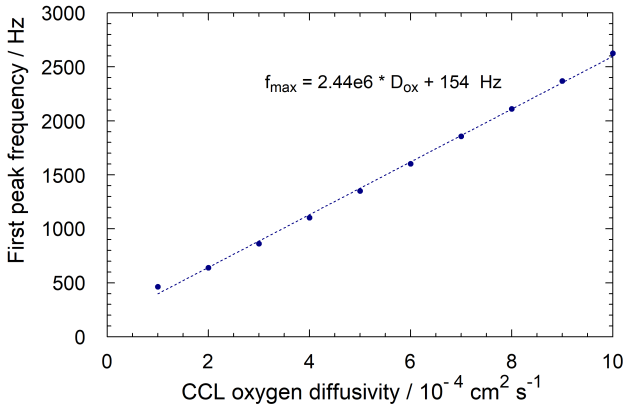

FIG. 4. Position of the first (leftmost) peak of $-\operatorname{Im}(\zeta^*_{ccl})$ (Figure 2b) on the frequency scale vs. CCL oxygen diffusivity D_{ox}.

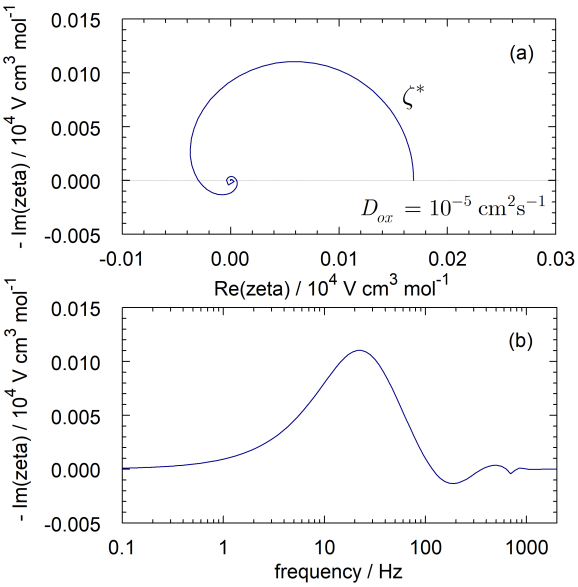

FIG. 5. (a) The Nyquist spectrum of ζ^* for $D_{ox} = 10^{-5}$ cm^2 s^{-1}. (b) The frequency dependence of imaginary part of impedance in (a).

and $1/\tilde{\zeta}_{ccl}$, respectively, at $\tilde{\omega}=0$. The first terms of expansion give

$$\tilde{\zeta}^0=\frac{2}{\tilde{c}_1^0}\left(\frac{\tilde{j}_0}{\tilde{j}_{ox}}\tanh\left(\frac{\tilde{j}_0}{\tilde{j}_{ox}}\right)+\frac{\tilde{D}_{ox}\tilde{l}_b}{\tilde{D}_b}\frac{\tilde{j}_0}{\tilde{j}_{ox}}\left(1+\frac{\tilde{j}_0}{\tilde{j}_{ox}}-\frac{\exp\left(-\tilde{j}_0/\tilde{j}_{ox}\right)}{\cosh\left(\tilde{j}_0/\tilde{j}_{ox}\right)}\right)\right)^{-1} \tag{30}$$

$$\tilde{\zeta}^0_{ccl}=\frac{2}{\tilde{c}_1^0\left(\tilde{j}_0/\tilde{j}_{ox}\right)\tanh\left(\tilde{j}_0/\tilde{j}_{ox}\right)} \tag{31}$$

As expected, Eq.(30) transforms to Eq.(31) in the limit of $\tilde{D}_b\to\infty$. In the dimension form, Eqs.(30), (31) read

$$\zeta^0=\frac{2b}{c_1^0}\left(\frac{j_0}{j_{ox}}\tanh\left(\frac{j_0}{j_{ox}}\right)+\frac{D_{ox}l_b}{D_bl_t}\frac{j_0}{j_{ox}}\left(1+\frac{j_0}{j_{ox}}-\frac{\exp\left(-j_0/j_{ox}\right)}{\cosh\left(j_0/j_{ox}\right)}\right)\right)^{-1} \tag{32}$$

$$\zeta^0_{ccl}=\frac{2b}{c_1^0\left(j_0/j_{ox}\right)\tanh\left(j_0/j_{ox}\right)} \tag{33}$$

Eqs.(32),(33) can be used to estimate the oxygen diffusion coefficients in the CCL and GDL from the static point of zeta–spectrum. For $j_0\gtrsim j_{ox}$, we may set $\tanh\left(j_0/j_{ox}\right)\simeq 1$ and from Eq.(33) it follows that $\zeta^0_{ccl}\sim j_{ox}\sim D_{ox}$. Moreover, lowering of D_{ox} lowers the second term in brackets in Eq.(32), and the dependence of ζ^0 on D_{ox} also tends to linear: $\zeta^0\sim D_{ox}$. This explains dramatic shrinking of ζ^0 Nyquist spectrum in Figure 5a as compared to Figure 2a.

In the limit of large oxygen consumption considered in this section, the right side of Eq.(19) is zero. It can be shown that in this limit, $\partial\tilde{A}/\partial\tilde{x}|_{\tilde{x}=0}=-1/\tilde{Z}$ and from Eq.(19) it follows that electric impedance $\tilde{Z}$ tends to impedance of a pure capacitor: $\tilde{Z}=1/(\mathrm{i}\tilde{\omega}\xi^2)$. Thus, electric impedance is of limited use in this regime, while zeta–impedance gives the cell oxygen transport parameters.

D. Qualitative comparison with experiment

Engebretsen et al.[2] measured pressure impedance spectra by applying acoustic signal to the PEMFC flow field. The data in[2] are reported as plots of absolute value and phase angle of pressure impedance vs. frequency. Figure 6 shows the data[2] recalculated as ζ–impedance using

$$\zeta=\frac{\delta\eta}{\delta c}=RT\frac{\delta V}{\delta p}=RT\left|\frac{\delta V}{\delta p}\right|\exp(\mathrm{i}\theta)$$

where δp is the amplitude of pressure perturbation applied to the cell, δV is the voltage response, and θ is the phase angle. The shape of model spectra in Figure 2 is similar to the shape of experimental spectrum in Figure 6. The spectrum in Figure 6 has been measured using the standard PEM fuel cell at $j_0=0.8$ A cm^{-2} and we demonstrate only qualitative resemblance of model and experimental spectra. Note that the spiral behavior of zeta–spectra at high frequencies has been reported in[3].

The model above is developed assuming fast proton transport in the CCL. This means that the cell current density must be much less than the characteristic current for proton transport in the CCL:

$$j_0\ll j_*=\frac{\sigma_p b}{l_t} \tag{34}$$

where σ_p is the CCL proton conductivity. In a working PEMFC, $\sigma_p\simeq 0.02$ S cm^{-1}, hence with $b=0.03$ V and $l_t=10\cdot10^{-4}$ cm we get $j_*=0.6$ A cm^{-2}. Thus, the optimal regime for measuring ζ in a cell would be close to the cell current density of about 100 mA cm^{-2}. On the other hand, Eq.(27) must hold for equations of this section to be valid. Fulfillment of Eq.(27) can be provided by lowering inlet oxygen concentration, in order for the working current density exceeded the oxygen–transport current density j_{ox}.

The model above assumes uniform static oxygen concentration, local current density and pressure along the channel. These conditions hold if stoichiometry of oxygen flow is high, the channel is short and the pressure perturbation is applied over the whole cathode flow field, as in experiments[2]. The model is not applicable for the cases of large pressure drop along the channel and/or low oxygen stoichiometry.

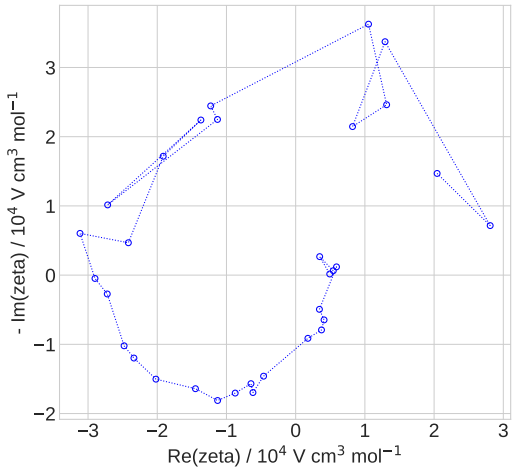

FIG. 6. The experimental Nyquist spectrum of ζ–impedance of a standard PEM fuel cell at the cell current of 0.8 A cm^{-2} (Ref.[2]). The absolute value of pressure impedance $|\delta V/\delta p|$ and the phase shift angle θ have been digitized from Figure 2 of Ref.[2]. Noisy curve is explained by poor accuracy of digitizing.

IV. CONCLUSIONS

We report analytical solutions for concentration (zeta–) impedance of a PEM fuel cell cathode. Oxygen transport in the catalyst and gas diffusion layers are taken into account; oxygen concentration over the whole active area is assumed to be constant (large stoichiometry of the air flow). The system of linear equations for the oxygen concentration perturbation amplitude in the porous layers is obtained by linearization and Fourier–transform of oxygen mass transport equations. The system is solved leading to the formula for the zeta–impedance $\zeta = \delta\eta/\delta c$. A formula relating ζ–impedance and standard "electric" impedance Z is obtained.

The solution for ζ contains free model parameter, the inverse value of zeta–impedance at the catalyst layer/membrane interface. In the limit of large oxygen consumption in the catalyst layer, this parameter can be set to zero, which gives simple relations for the zeta–impedance and for its static limit. The latter relation allows one to estimate oxygen transport parameters of the CCL and GDL from zeta–spectra. Qualitative resemblance of the model and experimental spectrum available in literature is demonstrated.

[1] A. M. Niroumand, W. Merida, M. Eikerling, and M. Saif. Pressure–voltage oscillations as a diagnostic tool for PEFC cathodes. *Electrochem. Comm.*, 12:122–124, 2010. doi:10.1016/j.elecom.2009.11.003.

[2] E. Engebretsen, T. J. Mason, P. R. Shearing, G. Hinds, and D. J. L. Brett. Electrochemical pressure impedance spectroscopy applied to the study of polymer electrolyte fuel cells. *Electrochem. Comm.*, 75:60–63, 2017. doi:10.1016/j.elecom.2016.12.014.

[3] A. Sorrentino, T. Vidakovic-Koch, R. Hanke-Rauschenbach, and K. Sundmacher. Concentration–alternating frequency response: A new method for studying polymer electrolyte membrane fuel cell dynamics. *Electrochim. Acta*, 243:53–64, 2017. doi:10.1016/j.electacta.2017.04.150.

[4] A. V. Shirsath, S. Rael, C. Bonnet, L. Schiffer, W. Bessler, and F. Lapicque. Electrochemical pressure impedance spectroscopy for investigation of mass transfer in polymer electrolyte membrane fuel cells. *Current Opinion in Electrochem.*, 20:82–87, 2020. doi:10.1016/j.coelec.2020.04.017.

[5] F. Kubannek and U. Krewer. Studying the interaction of mass transport and electrochemical reaction kinetics by species frequency response analysis. *J. Electrochem. Soc.*, 167:144510, 2020. doi:10.1149/1945-7111/abc76e.

[6] A. Sorrentino, T. Vidakovic-Koch, and K. Sundmacher. Studying mass transport dynamics in polymer electrolyte membrane fuel cells using concentration–alternating frequency response analysis. *J. Power Sources*, 412:331–335, 2019. doi:10.1016/j.jpowsour.2018.11.065.

[7] A. Kulikovsky. A model for concentration impedance of a PEM fuel cell. *eTrans.*, 2:100026, 2019. doi:10.1016/j.etran.2019.100026.

[8] Andrei Kulikovsky. "Corrigendum to "A model for concentration impedance of a pem fuel cell" [etrans (2019) 2 100026. doi: 10.1016/j.etran.2019.100026]. *eTrans.*, 7:100110, 2021. doi:10.1016/j.etran.2021.100110.

[9] A. Sorrentino, K. Sundmacher, and T. Vidakovic-Koch. Polymer electrolyte fuel cell degradation mechanisms and their diagnosis by frequency response analysis methods: A review. *Energies*, 13:5825, 2020. doi:10.3390/en13215825.

[10] M. Eikerling and A. A. Kulikovsky. *Polymer Electrolyte Fuel Cells: Physical Principles of Materials and Operation*. CRC Press, London, 2014.

[11] A. A. Kulikovsky. Analytical physics–based impedance of the cathode catalyst layer in a PEM fuel cell at typical working currents. *Electrochim. Acta*, 225:559–565, 2016. doi:10.1016/j.electacta.2016.11.129.

[12] A. Kulikovsky and O. Shamardina. A model for PEM fuel cell impedance: Oxygen flow in the channel triggers spatial and frequency oscillations of the local impedance. *J. Electrochem. Soc.*, 162:F1068–F1077, 2015. doi:10.1149/2.0911509jes.

[13] A. A. Kulikovsky. The regimes of catalyst layer operation in a fuel cell. *Electrochim. Acta*, 55:6391–6401, 2010.

[14] T. Reshetenko and A. Kulikovsky. Variation of PEM fuel cell physical parameters with current: Impedance spectroscopy study. *J. Electrochem. Soc.*, 163(9):F1100–F1106, 2016. doi:10.1149/2.0981609jes.

Nomenclature

$\tilde{}$	Marks dimensionless variables
A	Electric admittance, Ω^{-1}cm^{-2}
b	ORR Tafel slope, V
C_{dl}	Double layer volumetric capacitance, F cm^{-3}
c	Oxygen concentration in the CCL, mol cm^{-3}
c_b	Oxygen concentration in the GDL, mol cm^{-3}
c_1^0	Static oxygen concentration at the CCL/GDL interface, mol cm^{-3}
c_h	Oxygen concentration in the channel, mol cm^{-3}
c_h^{in}	Reference (inlet) oxygen concentration, mol cm^{-3}
D_b	Oxygen diffusion coefficient in the GDL, cm^2 s^{-1}
D_{ox}	Oxygen diffusion coefficient in the CCl, cm^2 s^{-1}
F	Faraday constant, C mol^{-1}
$\tilde{G}$	$= \tilde{c}^1/\tilde{\eta}^1$, dimensionless concentration admittance. Note that $\tilde{\zeta} = 1/\tilde{G}$
i_*	ORR volumetric exchange current density, A cm^{-3}
i	Imaginary unit
j	Local proton current density in the CCL, A cm^{-2}
j_{ox}	Characteristic current density of oxygen transport, A cm^{-2}, Eq.(27)
j_*	Characteristic current density of proton transport, A cm^{-2}, Eq.(34)
j_0	Cell current density, A cm^{-2}
l_b	GDL thickness, cm
l_t	CCL thickness, cm
x	Coordinate through the CCL and GDL, cm
Z	Electric impedance, Ω cm^2

Subscripts:

0	Membrane/CCL interface
1	CCL/GDL interface
ccl	Cathode catalyst layer
h	Channel
t	Catalyst layer

Superscripts:

0	Steady–state value
1	Small–amplitude perturbation
$*$	At large cell current

Greek:

α, β	Dimensionless auxiliary parameters, Eq.(7)
η	ORR overpotential, positive by convention, V
ζ	Concentration impedance, V cm^3 mol^{-1}
ϕ_0, ϕ_1	Auxiliary dimensionless parameters, Eq.(13)
σ_p	CCL proton conductivity, S cm^{-1}
ω	Angular frequency of the AC signal, s^{-1}